Polaron-phonon interaction in a finite-size lattice: A perturbative approach

Vincent Pouthier*
Institut UTINAM, Université de Franche-Comté, CNRS UMR 6213, FR-25030 Besançon Cedex, France
(Received 9 June 2011; revised manuscript received 30 August 2011; published 10 October 2011)

The finite-size exciton-phonon system is revisited within the small polaron theory. Two strategies are used to treat the polaron-phonon interaction. The interaction is first expanded as a Taylor series with respect to the coupling strength. It describes polaron scattering mediated by the exchange of real and virtual phonons, the latter resulting from phonon vacuum fluctuations. However, this method does not improve energy calculations when compared with standard second-order perturbation theory. A more accurate approach is obtained by using a normally order expansion of the interaction. The vacuum fluctuations are renormalized up to infinity and a polaron Hamiltonian is defined in terms of inhomogeneous effective hopping constants. Due to the finite size of the lattice, the polaron energy spectrum exhibits discrete energy levels that are red shifted owing to the polaron-phonon interaction. By contrast, each phonon frequency is either red or blue shifted depending on the nature of the state occupied by the polaron that accompanies the phonon. But the larger is the lattice size, the smaller is the phonon frequency shift. Finally, for odd lattice sizes, the phonon frequencies remain unchanged when the polaron occupies the band center.

DOI: 10.1103/PhysRevB.84.134301 PACS number(s): 71.35.−y, 71.38.−k, 63.22.−m, 03.65.Yz

I. INTRODUCTION

Quantum-state transfer (QST) from one region to another is a fundamental task in quantum computing.[1] Over short-length scales, to ensure communication inside a computer or between adjacent computers, solid-state based system is the ideal candidate for scalable quantum computing.[2] Because the quantum channel depends on the way the information is encoded, different strategies have been elaborated involving, for instance, optical lattices.[3] arrays of quantum dots,[4] and quantum spin networks.[5,6] However, it has been pointed out that qubits may be encoded on high-frequency vibrational modes.[7–9] Vibrational exciton-mediated QST is thus a promising way for quantum information processing.[10,11]

In that context, the dynamics of a finite-size exciton-phonon system has been recently studied.[12,13] Based on the Fröhlich model[14] (acoustic phonons), the nonadiabatic weak-coupling limit was considered, i.e., a common situation for vibrational excitons in molecular lattices such as adsorbed nanostructures[15–24] and biopolymers.[25–40] To investigate QST, special attention has been paid for describing coherences of the exciton reduced density matrix that measure the ability of the exciton to develop superimpositions involving the vacuum and one-exciton states. Because generalized master equation breaks down in finite-size lattices,[41] standard perturbation theory (PT) has been applied.

Within PT, the dynamics is governed by an effective Hamiltonian that takes exciton-phonon entanglement into account. The exciton is clothed by a virtual phonon cloud whereas the phonons are dressed by virtual excitonic transitions. In that case, quantum decoherence is encoded in the decoherence function[42,43] that provides information on the ability of the phonons to evolve freely in spite of the exciton-phonon coupling. At zero temperature, the phonons are in a pure state. The decoherence function reduces to a phase factor involving the frequency difference between free and dressed phonons. At finite temperature, an average procedure yields a sum over phase factors, which interfere with the others, resulting in the decay of the excitonic coherences. Consequently, temperature-enhanced quantum decoherence takes place. Nevertheless, when compared with infinite lattices,[44] the confinement softens the decoherence and allows high-fidelity QST.

The previous scenario[12,13] reveals that exciton-phonon interaction-induced phonon frequency shift is a key ingredient for understanding quantum decoherence. Unfortunately, our previous works were restricted to the weak-coupling limit. To go beyond this restriction, the finite-size exciton-phonon system is thus revisited within the polaron concept,[45–47] a more accurate approach for treating intermediate- and strong-coupling regimes. In the nonadiabatic limit, this approach involves the Lang-Firsov (LF) transformation that partially removes the exciton-phonon interaction.[48] A new point of view is generated in which the elementary excitation is no longer a bare exciton but a small polaron, i.e., an exciton dressed by a lattice distortion. The dressing modifies the exciton energy but it does not affect the phonon frequency.

In fact, LF is not exact and a polaron-phonon coupling remains. It turns out that before the 2000s, most of the works focused on the influence of the polaron-phonon interaction on the polaron properties. Only few studies were performed to understand the way this interaction modifies the phonon frequency.[49,50] Fortunately, Ivic and co-workers have recently developed several methods to characterize the modification of the phonon spectra in infinite lattices with translational invariance.[51–54] They showed that the polaron-phonon interaction yields either the softening or the hardening of the phonon frequency, depending on the sign of the exciton hopping constant.

Quite naturally, in the present work, we address a detailed study by combining LF and PT to understand what is happening in a finite-size lattice. It will be shown that the polaron energy spectrum exhibits discrete energy levels that are red shifted owing to the polaron-phonon interaction. Similarly, each phonon experiences a frequency shift when it is accompanied by a polaron. This effect is an intrinsic property of a confined lattice because the larger is the lattice

size, the smaller is the shift. Whatever the sign of the exciton hopping constant, the polaron-phonon interaction leads either to the softening or to the hardening of the phonon frequency, depending on the state occupied by the polaron. However, for odd lattice sizes, the phonon frequencies remain unchanged when the polaron exactly lies at the band center.

The paper is organized as follows. In Sec. II, the finite-size exciton-phonon system is described and the results provided by PT are briefly summarized. Then, the small-polaron point of view is introduced in Sec. III. Two different strategies to treat the polaron-phonon interaction are presented in Secs. IV and V, respectively. Finally, numerical calculations are carried out and discussed in Sec. VI.

II. FINITE-SIZE EXCITON-PHONON SYSTEM

As detailed in numerous papers,[12,13,39,41] the exciton-phonon properties in a finite-size lattice containing N sites $x = 1, \ldots, N$ are governed by the Hamiltonian

$$H = \omega_0 I_A + \Phi\mathcal{T} + \sum_{p=1}^{N} \Omega_p a_p^\dagger a_p + \sum_{p=1}^{N} M_p (a_p^\dagger + a_p). \quad (1)$$

The first two terms define the exciton Hamiltonian H_A that characterizes the dynamics of N coupled two-level systems with Bohr frequency ω_0. It is defined in terms of the exciton potential energy $\omega_0 I_A$, where I_A is the identity operator in the one-exciton subspace $\mathcal{E}_A$. The contribution $\Phi\mathcal{T}$ denotes the kinetic energy that describes the delocalization of the exciton between neighboring sites. It involves the bare hopping constant Φ and the Hermitian transfer matrix $\mathcal{T}$ defined as

$$\mathcal{T} = \sum_{x=1}^{N-1} |x+1\rangle\langle x| + |x\rangle\langle x+1|, \quad (2)$$

where $|x\rangle$ is the first excited state of the xth two-level system. Owing to the confinement, the exciton eigenstates are stationary waves with quantized wave vectors $K_k = k\pi/L$, with $k = 1, \ldots, N$ and $L = N + 1$, as

$$|k\rangle = \sum_{x=1}^{N} \sqrt{\frac{2}{L}} \sin(K_k)|x\rangle. \quad (3)$$

The corresponding eigenenergies $\omega_k = \omega_0 + 2\Phi\cos(K_k)$ form a symmetric ladder of N discrete energy levels that belong to a band centered on ω_0 and whose width is approximately 4Φ. The third term in Eq. (1) is the phonon Hamiltonian H_B. It describes the external motions of the lattice sites viewed as point masses M connected via force constants W. With fixed boundary conditions, the phonons correspond to N stationary normal modes with quantized wave vectors $q_p = p\pi/L$, with $p = 1, \ldots, N$. The associated frequencies are $\Omega_p = \Omega_c \sin(q_p/2)$ with $\Omega_c = \sqrt{4W/M}$. In the phonon Hilbert space $\mathcal{E}_B$, the dynamics is described in terms of the standard phonon operators $a_p^\dagger$ and a_p and the eigenstates are well-known phonon number states $|\{n_p\}\rangle = |n_1, n_2, \ldots, n_p\rangle$. The last term in Eq. (1) is the exciton-phonon interaction ΔH that acts in $\mathcal{E}_A \otimes \mathcal{E}_B$. It involves the Hermitian operator M_p that measures the coupling strength between the exciton and the pth phonon mode. The interaction yields a stochastic modulation of each two-level system Bohr frequency by the lattice vibrations. In the local basis $\{|x\rangle\}$, M_p is thus represented by a diagonal matrix as

$$M_{pxx'} = 2\eta_p \cos(q_p x)\delta_{xx'}, \quad (4)$$

where $\eta_p = [(E_B\Omega_p/L)(1 - (\Omega_p/\Omega_c)^2)]^{1/2}$ is the modulation amplitude induced by the pth phonon mode, E_B being the small-polaron binding energy. In the exciton eigenbasis $\{|k\rangle\}$, M_p is no longer diagonal and its elements are expressed as

$$M_{pkk'} = \eta_p(\delta_{p,k-k'} + \delta_{p,k'-k} - \delta_{p,k+k'} - \delta_{p,2L-k-k'}). \quad (5)$$

Equation (5) shows that ΔH favors exciton scattering from state $|k\rangle$ with energy ω_k, to state $|k'\rangle$ with energy $\omega_{k'}$ via the exchange of a phonon p with energy Ω_p. The allowed transitions are specified by the selection rules $M_{pkk'} \neq 0$ that generalize the concept of momentum conservation in a finite-size lattice.

In the nonadiabatic ($4\Phi < \Omega_c$) weak-coupling ($E_B \ll \Phi$) limit, it has been shown that standard PT is particularly suitable to solve H and to highlight exciton-phonon entanglement.[12,13] ΔH being a small perturbation, the unperturbed states $|k\rangle \otimes |\{n_p\}\rangle$ refer to a free exciton accompanied by free phonons. Although ΔH favors transitions between unperturbed states, it turns out that there is no resonance between coupled unperturbed states. PT was thus used to evaluate energy corrections up to second-order in ΔH. Therefore, in a state $|k\rangle$, the energy of an exciton $\hat{\omega}_k = \omega_k + \delta\omega_k^{(0)}$ is renormalized due to its coupling with the phonons. Similarly, each phonon of the pth mode experiences a frequency shift $\delta\Omega_{pk}^{(0)}$ when it is accompanied by an exciton in state $|k\rangle$. The energy corrections are defined as

$$\begin{aligned} \delta\omega_k^{(0)} &= \sum_{p=1}^{N}\sum_{k'=1}^{N} \frac{M_{pkk'}^2}{\omega_k - \omega_{k'} - \Omega_p}, \\ \delta\Omega_{pk}^{(0)} &= \sum_{k'=1}^{N} \frac{2M_{pkk'}^2(\omega_k - \omega_{k'})}{(\omega_k - \omega_{k'})^2 - \Omega_p^2}. \end{aligned} \quad (6)$$

Because no resonance occurs in the nonadiabatic limit, Eq. (6) reveals that the exciton is dressed by a virtual phonon cloud whereas each phonon is clothed by virtual excitonic transitions. Unfortunately, it provides a quite good description of the exciton-phonon dynamics in the weak-coupling limit, only. To go beyond and to investigate intermediate- and strong-coupling regimes, a small polaron approach is developed in the following sections.

III. THE SMALL POLARON POINT OF VIEW

The polaron concept arises through the assumption that the interaction ΔH predominates over the kinetic energy $\Phi\mathcal{T}$. The system Hamiltonian is thus rewritten as

$$H = H_0' + V, \quad (7)$$

where $V = \Phi\mathcal{T}$ whereas H_0' reduces to H in the limit $\Phi = 0$. It describes an immobile exciton coupled with confined phonons and exhibits a local character owing to the diagonal representation of M_p in the local basis [Eq. (4)]. In that context,

LF is the unitary transformation U that exactly removes ΔH in the limit $\Phi = 0$, as

$$U = \sum_{x=1}^{N} \theta_x^\dagger |x\rangle\langle x|, \tag{8}$$

where the dressing operator θ_x is the representation of a general operator defined as

$$\theta = \exp\left(-\sum_{p=1}^{N} \Lambda_p A_p\right). \tag{9}$$

In Eq. (9), $\Lambda_p = M_p/\Omega_p$ defines the Hermitian coupling operator that acts in $\mathcal{E}_A$. Isomorphic to M_p, it is diagonal in the local basis. By contrast, $A_p = a_p^\dagger - a_p$ is an anti-Hermitian phonon operator that acts in $\mathcal{E}_B$. Note that $[\Lambda_p, \Lambda_{p'}] = 0$, $[A_p, A_{p'}] = 0$, and $[\Lambda_p, A_{p'}] = 0\ \forall p, p'$.

By applying LF, $\tilde{H}_0' = U H_0' U^\dagger$ becomes diagonal in the local basis $|x\rangle \otimes |\{n_p\}\rangle$, as

$$\tilde{H}_0' = \sum_{x=1}^{N} (\omega_0 - \epsilon_x)|x\rangle\langle x| + H_B, \tag{10}$$

where $\epsilon_x = \sum_{p=1}^{N} M_{pxx}^2/\Omega_p$. Because LF conserves eigenvalues, both H_0' and $\tilde{H}_0'$ exhibit the same energy spectrum. However, the eigenstates of H_0' differ from those of $\tilde{H}_0'$ and they are defined as $|x\rangle \otimes \theta_x|\{n_p\}\rangle$.

LF generates a new point of view in which $|x\rangle$ no longer refer to an exciton localized on the xth two-level system. Instead, it defines an immobile small polaron, i.e., an exciton dressed by a virtual phonon cloud. The dressing favors a redshift ϵ_x of the xth two-level system Bohr frequency. With fixed boundary conditions, it turns out that this shift is site independent, i.e., $\epsilon_x = \epsilon_B\ \forall x$. Nevertheless, it depends on the lattice size so that the modified Bohr frequency becomes $\tilde{\omega}_0 = \omega_0 - \epsilon_B$ with $\epsilon_B = E_B(1 - 2/L)$. In the new point of view, the phonon frequencies remain identical to those of unperturbed phonons. Nevertheless, the polaron formation affects the phonon eigenstates. For each phonon mode, they behave as coherent quasiclassical states that depend on the exciton position. These coherent states define the virtual phonon cloud that surrounds the exciton, namely, the so-called lattice distortion, and they partially take exciton-phonon entanglement into account.

When the exciton is allowed to move, the polaron-phonon dynamics is governed by the transformed Hamiltonian $\tilde{H} = U H U^\dagger$ defined as

$$\tilde{H} = \tilde{\omega}_0 I_A + H_B + \Phi\theta^\dagger \mathcal{T}\theta. \tag{11}$$

When $\Phi \neq 0$, LF partially removes the interaction and a polaron-phonon coupling, $\tilde{V} = \Phi\theta^\dagger\mathcal{T}\theta$ remains. This coupling favors polaronic transitions between neighboring sites, either freely or through phonon exchanges. It is as if the polaron exhibited hopping constants that randomly fluctuate owing to the lattice motions.

Therefore, within the small-polaron point of view, a major problem rapidly occurs. How to intelligently split $\tilde{H}$ to treat efficiently the polaron-phonon interaction? To answer that question the so-called $1/\lambda$ expansion has been used by Alexandrov and co-workers[46,47] for an infinite lattice and in the strong-coupling limit ($\lambda = E_B/2\Phi$). Within this method, the first two terms in Eq. (11) define an unperturbed Hamiltonian, whereas $\tilde{V}$ is addressed using second order perturbation theory. In the present paper, an alternative approach is used to investigate weak-, intermediate-, and strong-coupling regimes. Quite simple, it is based on the expansion of $\tilde{V}$ in terms of the exciton-phonon coupling strength. Although such a procedure may appear less accurate than other methods, it has the advantage to remove a certain arbitrariness to better control the invoked approximations. In doing so, it turns out that $\tilde{V}$ can be expanded in two different ways, called the standard expansion (SE) and the normally ordered expansion (NOE), respectively. As shown in the next two sections, SE yields results quite similar to those obtained within standard PT (weak-coupling regime), whereas NOE allows to investigate intermediate- and strong-coupling regimes.

IV. STANDARD EXPANSION

Within SE, $\tilde{V} = \Phi\theta^\dagger\mathcal{T}\theta$ is expanded by using the well-known Baker-Hausdorff formula.[55] After straightforward algebraic manipulations, one finally obtains $\tilde{V} = \sum_{m=0}^{\infty} \tilde{V}_m$ with

$$\tilde{V}_m = \sum_{p_1}\sum_{p_2}\cdots\sum_{p_m} \tilde{V}_{m,p_1p_2\ldots p_m} A_{p_1} A_{p_2}\cdots A_{p_m}, \tag{12}$$

and

$$\tilde{V}_{m,p_1p_2\ldots p_m} = \frac{\Phi}{m!}[\Lambda_{p_1},[\Lambda_{p_2},\ldots.[\Lambda_{p_m},\mathcal{T}]\cdots]]. \tag{13}$$

Because Λ_p measures the exciton-phonon coupling strength, SE is clearly a perturbative expansion. At lowest order, $\tilde{V}_0 = \Phi\mathcal{T}$ is the kinetic energy of a bare exciton. By adding this term to $\tilde{\omega}_0 I_A$, we can define a new polaron Hamiltonian that includes both potential and kinetic energy effects:

$$H_{\rm po} = \tilde{\omega}_0 I_A + \Phi\mathcal{T}. \tag{14}$$

The polaron-phonon Hamiltonian is thus split as

$$\tilde{H} = \tilde{H}_0 + \tilde{V}_1 + \tilde{V}_2 + \cdots, \tag{15}$$

where $\tilde{H}_0 = H_{\rm po} + H_B$ is the unperturbed polaron-phonon Hamiltonian.

As shown in Eq. (14), $H_{\rm po}$ is isomorphic to the exciton Hamiltonian H_A [Eq. (1)]. The polaron eigenstates are thus stationary states $|k\rangle$ whose eigenvalues $\tilde{\omega}_k = \tilde{\omega}_0 + 2\Phi\cos(K_k)$ are red shifted by on amount equal to ϵ_B when compared with the corresponding excitonic eigenenergies. By contrast, the phonon frequencies remain unchanged. Therefore the unperturbed states $|k\rangle \otimes |\{n_p\}\rangle$ refer to a free polaron accompanied by free phonons, polaron, and phonons being independent. Note that it should be keep in mind that although they factorize, the unperturbed states take exciton-phonon entanglement into account via the dressing effect that results form LF.

To first order, the interaction is written as

$$\tilde{V}_1 = \sum_{p=1}^{N} \tilde{V}_{1,p} a_p^\dagger + \tilde{V}_{1,p}^\dagger a_p, \tag{16}$$

where $\tilde{V}_{1,p} = \Phi[\Lambda_p, \mathcal{T}]$ is an anti-Hermitian operator whose matrix elements are defined as

$$\langle k|\tilde{V}_{1,p}|k'\rangle = \frac{\tilde{\omega}_{k'} - \tilde{\omega}_k}{\Omega_p} M_{pkk'}. \tag{17}$$

$\tilde{V}_1$ favors polaron scattering from $|k\rangle$ to $|k'\rangle$ via the exchange of a real phonon p. The allowed transitions satisfy selection rules similar to those connected to the exciton-phonon problem ($M_{pkk'} \neq 0$) excepted that diagonal terms vanish ($\langle k|\tilde{V}_{1,p}|k\rangle = 0$). However, the key point concerns the strength of the interaction. Indeed, as pointed out in Refs. 12 and 13, the phonon mode $p = 1$ yields the largest perturbation. This perturbation affects polaronic states located close to the band center so that one approximately obtains $\langle k|\tilde{V}_{1,p}|k'\rangle \approx 2BM_{pkk'}$. For $B \ll 1$, $\tilde{V}_1$ appears smaller than ΔH suggesting that PT is *a priori* more accurate after performing LF.

To second order, the interaction is written as

$$\tilde{V}_2 = \sum_{p,p'=1}^{N} \tilde{V}_{2,pp'}(a_p a_{p'} + a_p^\dagger a_{p'}^\dagger - a_p^\dagger a_{p'} - a_p a_{p'}^\dagger), \tag{18}$$

where $\tilde{V}_{2,pp'} = \Phi[\Lambda_p, [\Lambda_{p'}, \mathcal{T}]]/2$ is a hHermitian matrix. As shown in Eq. (18), $\tilde{V}_2$ exhibits four contributions whose physics can be explained as follows. According to the first contribution (term $a_p a_{p'}$), a polaron $|k\rangle$ and two phonons p and p' first propagate freely. Then, owing to the interaction, the polaron is scattered in $|k'\rangle$, whereas the two phonons are absorbed. The second contribution (term $a_p^\dagger a_{p'}^\dagger$) is the complementary process during which the polaron scattering results from the emission of the two phonons. The third contribution (term $a_p^\dagger a_{p'}$) first describes the free evolution of a polaron accompanied by a phonon p'. Then, the phonon p' is absorbed and the phonon p is emitted giving rise to polaron scattering. Finally, it turns out that the last contribution (term $a_p a_{p'}^\dagger$) is not the complementary process of the third contribution. Although it still refers to polaron scattering, it is as if the phonon p' was emitted spontaneously before the interaction and that the phonon p was absorbed long after the coupling. To overcome this problem and obtain a coherent scenario, $\tilde{V}_2$ must be normally ordered. To proceed, all creation phonon operators are moved to the left of all annihilation phonon operators by using the phonon commutation rules. $\tilde{V}_2$ is thus rewritten as

$$\tilde{V}_2 = \sum_{p,p'=1}^{N} \tilde{V}_{2,pp'}(a_p a_{p'} + a_p^\dagger a_{p'}^\dagger - a_p^\dagger a_{p'} - a_{p'}^\dagger a_p - \delta_{pp'}).$$

In normal order, the first four contributions define complementary processes that characterize polaron scattering mediated by the exchange of real phonons. However, a fifth contribution occurs. Independent on the phonon operators, it originates in the phonon vacuum fluctuations. These fluctuations favor processes during which a virtual phonon is emitted and spontaneously reabsorbed, giving rise to polaron scattering. They thus provide a correction to H_{po} equal to $\langle 0_B|\tilde{V}_2|0_B\rangle$, $|0_B\rangle$ denoting the phonon vacuum state.

We have verified that the previous scenario generalizes to high-order contributions. By using Wick's theorem,[45] it turns out that $\tilde{V}_m$ can be reorganized as the sum of normally order contributions. The rth component of the sum describes polaron scattering mediated by the exchange of r real phonons, $(m - r)/2$ virtual phonons being emitted and spontaneously reabsorbed owing to phonon vacuum fluctuations.

In that context, SE provides a starting point to apply PT for evaluating energy corrections. Up to second-order, the energy of a polaron in state $|k\rangle$ is renormalized due to its coupling with the phonons. The energy correction exhibits two contributions $\delta\tilde{\omega}_k = \delta\tilde{\omega}_k^{(1)} + \delta\tilde{\omega}_k^{(2)}$ as

$$\begin{aligned} \delta\tilde{\omega}_k^{(1)} &= \sum_{p=1}^{N}\sum_{k'=1}^{N} \left(\frac{\tilde{\omega}_k - \tilde{\omega}_{k'}}{\Omega_p}\right)^2 \frac{M_{pk'k}^2}{\tilde{\omega}_k - \tilde{\omega}_{k'} - \Omega_p}, \\ \delta\tilde{\omega}_k^{(2)} &= -\sum_{p=1}^{N}\sum_{k'=1}^{N} \left(\frac{\tilde{\omega}_k - \tilde{\omega}_{k'}}{\Omega_p}\right) \frac{M_{pk'k}^2}{\Omega_p}. \end{aligned} \tag{19}$$

The correction $\delta\tilde{\omega}_k^{(1)}$ results form the interaction $\tilde{V}_1$. It originates in the spontaneous emission of a phonon p in the course of which the polaron realizes a transition from $|k\rangle$ to $|k'\rangle$. Provided that $B < 1/2$, the energy is not conserved during the transition so that the phonon emission is not a real process.[12,13] The polaron is only able to exchange a phonon, which is first emitted and then immediately reabsorbed. The exchanged phonon behaves as a virtual phonon that forms a virtual cloud, which accompanies the polaron during its propagation. By contrast, $\delta\tilde{\omega}_k^{(2)}$ results from the interaction $\tilde{V}_2$ that favors the emission of a true virtual phonon that is spontaneously reabsorbed. This phonon yields an additional virtual cloud that clothes the polaron during its propagation and renormalizes its energy.

When the polaron occupies a state $|k\rangle$, each phonon of the pth mode experiences a frequency shift $\delta\Omega_{pk} = \delta\Omega_{pk}^{(1)} + \delta\Omega_{pk}^{(2)}$, defined as

$$\begin{aligned} \delta\Omega_{pk}^{(1)} &= 2\sum_{k'=1}^{N} \left(\frac{\tilde{\omega}_k - \tilde{\omega}_{k'}}{\Omega_p}\right)^2 \frac{M_{pk'k}^2(\tilde{\omega}_k - \tilde{\omega}_{k'})}{(\tilde{\omega}_k - \tilde{\omega}_{k'})^2 - \Omega_p^2}, \\ \delta\Omega_{pk}^{(2)} &= -2\sum_{k'=1}^{N} \left(\frac{\tilde{\omega}_k - \tilde{\omega}_{k'}}{\Omega_p}\right) \frac{M_{pk'k}^2}{\Omega_p}. \end{aligned} \tag{20}$$

The shift $\delta\Omega_{pk}^{(1)}$, due to $\tilde{V}_1$, results from two mechanisms. First, the phonon p can be absorbed giving rise to polaronic transitions from $|k\rangle$ to $|k'\rangle$. Such a process does not conserve the energy provided that $B < 1/2$ so that the phonon is immediately reemitted. Second, the phonon p can induce the stimulated emission of a second phonon during which the polaron realizes transitions, but the emitted phonon is immediately reabsorbed. Both mechanisms indicate that the phonon does no longer evolve freely but is dressed by virtual polaronic transitions. By contrast, $\delta\Omega_{pk}^{(2)}$ results from the diagonal contribution of $\tilde{V}_2$ that involves the phonon number operators. It turns on because the expectation value of this contribution does not vanish when the polaron occupies the state $|k\rangle$.

At this step, a quite surprising feature occurs. Indeed, after simple algebraic manipulations, it turns out that $\delta\omega_k^{(0)} = -\epsilon_B + \delta\tilde{\omega}_k^{(1)} + \delta\tilde{\omega}_k^{(2)}$ and $\delta\Omega_{pk}^{(0)} = \delta\Omega_{pk}^{(1)} + \delta\Omega_{pk}^{(2)}$. Although LF partially removes the exciton-phonon interaction, SE combined with PT does not improve the energy calculations when

compared with standard PT applied in the original exciton-phonon point of view. Up to second order in the exciton-phonon interaction, the polaron eigenenergies are identical to the exciton eigenenergies. Similarly, the phonon-frequency shifts are the same whether one works in the original or in the small-polaron point of view. However, it is worth mentioning that within the polaron point of view a better description of the system quantum states is obtained because exciton-phonon entanglement is already partially included by using LF. This is the reason why PT is more efficient in the polaron point of view.

V. NORMALLY ORDERED EXPANSION

As point out in Sec. IV, the mth contribution of SE accounts for polaron scattering induced by the exchange of m real phonons. In addition, owing to phonon vacuum fluctuations, it partially renormalizes processes in the course of which $m-2, m-4, \ldots$ real phonons are exchanged. The renormalization results from the emission of virtual phonons that are spontaneously reabsorbed. Consequently, it seems possible to obtain an alternative to SE in which the order no longer refer to the coupling strength but specifies the number of real phonon exchanged. Within this approach, called the normally ordered expansion (NOE) of the polaron-phonon interaction, the mth contribution describes all the processes involving m real phonons and either zero, one, two, etc. virtual phonons.

Starting from SE, NOE is formally obtained using normal ordering. However, this approach provides a perturbative expansion in terms of renormalized quantities. To perform an exact resummation, it is more efficient to apply normal ordering to the original expression of the polaron-phonon interaction represented in the local basis $\{|x\rangle\}$ [Eq. (11)]. As detailed in Appendix A, $\tilde{V}$ is written as $\tilde{V}=\sum_{m=0}^{\infty}\tilde{W}_m$. The mth contribution of the expansion is defined as

$$\tilde{W}_m=\sum_{p_1}\sum_{p_2}\cdots\sum_{p_m}\tilde{W}_{m,p_1p_2\ldots p_m}:A_{p_1}A_{p_2}\cdots A_{p_m}:, \tag{21}$$

where the double dot operation means normal ordering without taking into account of the commutation relation of the phonon operators. The operator $\tilde{W}_{m,p_1p_2Ap_m}$ that acts in $\mathcal{E}_A$ only, is written as

$$\tilde{W}_{m,p_1p_2\ldots p_m}=\frac{\Phi}{m!}[\Lambda_{p_1},[\Lambda_{p_2},\ldots[\Lambda_{p_m},\bar{\mathcal{T}}]\cdots]], \tag{22}$$

where $\bar{\mathcal{T}}$ is the effective transfer matrix defined as

$$\bar{\mathcal{T}}=\sum_{x=1}^{N-1}e^{-\sum_p\frac{1}{2}\lambda_{px}^2}(|x+1\rangle\langle x|+|x\rangle\langle x+1|). \tag{23}$$

with $\lambda_{px}=\Lambda_{px+1x+1}-\Lambda_{pxx}$.

Within NOE, $\tilde{W}_m$ describes polaron scattering mediated by the exchange of m real phonons. The scattering strength is renormalized up to infinity by taking into account exactly of the phonon vacuum fluctuations. The influence of these fluctuations is encoded in the effective transfer matrix defined as $\bar{\mathcal{T}}=\langle 0_B|\theta^\dagger\mathcal{T}\theta|0_B\rangle$.

Inserting NOE into Eq. (11) yields an alternative partition of the system Hamiltonian as

$$\tilde{H}=\tilde{\omega}_0 I_A+H_B+\tilde{W}_0+\tilde{W}_1+\tilde{W}_2+\cdots. \tag{24}$$

At lowest order, $\tilde{W}_0=\Phi\bar{\mathcal{T}}$ is an operator acting in $\mathcal{E}_A$, only. By adding this operator to the local term $\tilde{\omega}_0 I_A$, one obtains a new polaron Hamiltonian written as

$$\mathcal{H}_{\rm po}=\tilde{\omega}_0 I_A+\Phi\bar{\mathcal{T}}. \tag{25}$$

The polaron-phonon system Hamiltonian is thus split as

$$\tilde{H}=\tilde{\mathcal{H}}_0+\tilde{W}_1+\tilde{W}_2+\cdots, \tag{26}$$

where $\tilde{\mathcal{H}}_0=\mathcal{H}_{\rm po}+H_B$ is the new unperturbed polaron-phonon Hamiltonian.

The polaron Hamiltonian $\mathcal{H}_{\rm po}$ is no longer isomorphic to the exciton Hamiltonian because the kinetic energy involves the effective transfer matrix. This matrix accounts for the delocalization of the polaron owing to direct couplings between neighboring two-level systems. It also includes the influence of the vacuum fluctuations that favor polaronic hops mediated by the emission of virtual phonons that are spontaneously reabsorbed. Consequently, the motion of the polaron is governed by site dependent effective hopping constants that are smaller than the bare hopping constant. The hopping constant that connects two sites x and $x+1$ is defined as $\tilde{\Phi}_x=\Phi\exp(-S_x)$, where $S_x=\sum_{p=1}^{N}\lambda_{px}^2/2$ is the inhomogeneous band-narrowing factor.[46] Owing to this inhomogeneity, the polaronic eigenstates $|\mu\rangle$ and the associated eigenenergies $\tilde{\omega}_\mu$ no longer refer to stationary waves. They must be evaluated numerically, as illustrated in the next section.

Within NOE, the unperturbed states $|\mu\rangle\otimes|\{n_p\}\rangle$ describe a free polaron accompanied by free phonons, polaron, and phonons being independent. Therefore by treating $\tilde{W}_1$ at second order and $\tilde{W}_2$ at first order, second-order PT can be applied to evaluate the energy corrections. When compared with SE, this procedure allows the exact resummation of some contributions up to infinity in the exciton-phonon coupling strength through the dependence of both $\tilde{W}_m$ and $\mathcal{H}_{\rm po}$ in the effective transfer matrix. In that context, it is easy to show that the energy of a polaron in a state $|\mu\rangle$ is renormalized due to its coupling with the phonons. The energy correction is defined as

$$\delta\tilde{\omega}_\mu=\sum_{p=1}^{N}\sum_{\mu'=1}^{N}\left(\frac{\tilde{\omega}_\mu-\tilde{\omega}_{\mu'}}{\Omega_p}\right)^2\frac{M_{p\mu'\mu}^2}{\tilde{\omega}_\mu-\tilde{\omega}_{\mu'}-\Omega_p}, \tag{27}$$

where $\delta\tilde{\omega}_\mu$ originates in the interaction $\tilde{W}_1$. It describes energy correction induced by the spontaneous emission of a phonon p in the course of which the polaron realizes a transition from $|\mu\rangle$ to $|\mu'\rangle$. However, because polaron eigenstates no longer refer to stationary states, the allowed transitions satisfy new selection rules $M_{p\mu'\mu}\neq 0$. These selection rules differ from those that arise in the SE approach. At this step, there is no evidence that the energy is not conserved during a transition, even if the nonadiabatic limit is reached. Energy conservation during the polaron scattering may occur giving rise to PT break down. This fundamental point will be illustrated in the next section. Note that $\tilde{W}_2$ does not contribute to the correction

because the influence of the phonon vacuum fluctuations has already been taken into account.

Similarly, when the polaron occupies a state $|\mu\rangle$, each phonon of the pth mode experiences a frequency shift $\delta\Omega_{p\mu} = \delta\Omega^{(1)}_{p\mu} + \delta\Omega^{(2)}_{p\mu}$, defined as

$$\delta\Omega^{(1)}_{p\mu} = 2\sum_{\mu'=1}^{N}\left(\frac{\tilde{\omega}_\mu - \tilde{\omega}_{\mu'}}{\Omega_p}\right)^2 \frac{M^2_{p\mu'\mu}(\tilde{\omega}_\mu - \tilde{\omega}_{\mu'})}{(\tilde{\omega}_\mu - \tilde{\omega}_{\mu'})^2 - \Omega_p^2},$$
$$\delta\Omega^{(2)}_{p\mu} = -2\sum_{\mu'=1}^{N}\left(\frac{\tilde{\omega}_\mu - \tilde{\omega}_{\mu'}}{\Omega_p}\right)\frac{M^2_{p\mu'\mu}}{\Omega_p}. \quad (28)$$

The shift $\delta\Omega^{(1)}_{p\mu}$ originates in the interaction $\tilde{W}_1$. It results from the fact that the phonon p can either be absorbed or induce the stimulated emission of a second phonon, both processes being accompanied by the polaron scattering from $|\mu\rangle$ to $|\mu'\rangle$. By contrast, $\delta\Omega^{(2)}_{p\mu}$ originates in the diagonal contribution of $\tilde{W}_2$ that involves the phonon number operator $a^\dagger_p a_p$. It switches on because the expectation value of this contribution does not vanish when the polaron occupies the state $|\mu\rangle$.

Finally, allowing the renormalization of the phonon vacuum fluctuations up to infinity, NOE combined with standard PT appears more accurate than SE to evaluate energy corrections. However, numerical calculations are required for characterizing the polaron eigenstates $|\mu\rangle$ and the coupling matrix elements $M_{p\mu'\mu}$. These calculations are carried out in the next section where Eqs.(27) and (28) are computed.

VI. NUMERICAL RESULTS AND DISCUSSION

In this section, the previous formalism is applied for describing polaron-phonon interaction-induced energy corrections in a finite-size lattice. To proceed, the adiabaticity $B = 2\Phi/\Omega_c$ is fixed to 0.16, a common value for vibrational exciton.[12,13] Then, one defines $C = \Delta_0/2\Phi$ as the measure of the coupling strength, with $\Delta_0^2 = E_B\Omega_c/2$.[29] As shown in Sec. IV, SE yields energy corrections identical to those provided by PT applied in the original exciton-phonon point of view. Because these corrections have already been discussed,[12,13] special attention will be paid for describing results provided by NOE.

The first step consists in characterizing the eigenstates of $\mathcal{H}_{\rm po}$ [Eq. (25)] whose properties depend on the effective transfer matrix elements $\bar{\mathcal{T}}(x,x+1) = \exp(-S_x)$ [Eq. (23)]. As shown in Fig. 1, these elements behave as in an infinite lattice. They decrease as C increases and they approximately scale as $\exp(-S_\infty)\ \forall x$, where $S_\infty = 8E_B/3\pi\Omega_c$ is the band-narrowing factor in an infinite lattice. Nevertheless, Fig. 1 reveals that $\exp(-S_x)$ slightly depends on x. Indeed, as illustrated in Fig. 2, the dressing effect is enhanced near the lattice sides resulting in an inhomogeneous band-narrowing factor. Quite large on the side sites $x = 1$ and $x = N-1$, S_x decreases gradually as one reaches the core of the lattice. It reaches a minimum at the center of the lattice whose value $S_{L/2}$, that depends on the lattice size, is always larger than S_∞. Note that $S_{L/2}$ tends to S_∞ when $L \to \infty$. Consequently, the polaron is characterized by effective hopping constants $\tilde{\Phi}_x$ that are approximately $\tilde{\Phi} = \Phi\exp(-S_\infty)$ in the core of the lattice but slightly smaller close to the lattice sides, i.e.,

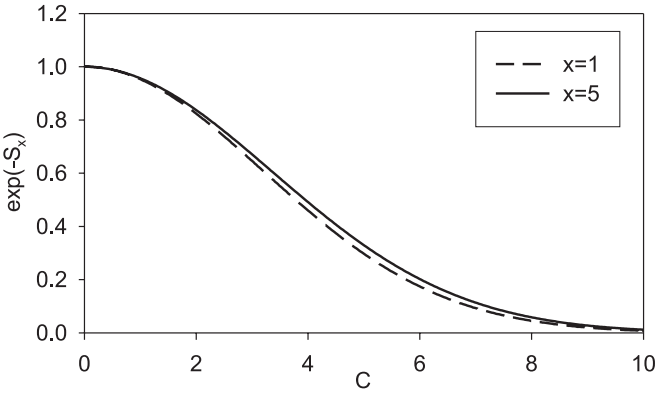

FIG. 1. $\bar{\mathcal{T}}(x,x+1)$ vs C for $N = 11$.

$\tilde{\Phi}_1 = \tilde{\Phi}_{N-1} < \tilde{\Phi}_{L/2}$. Note that this inhomogeneous character is enhanced by both L and C. Nevertheless, the inhomogeneity converges to a constant value provided that $N > 20$ for which $S_1 - S_{L/2} \approx 0.105 \times S_\infty$.

By using Eq. (4), straightforward calculations yield $S_x = S_\infty[F_L(x) + F_L(N-x)]$, where $F_L(x)$ is defined as

$$F_L(x) = \frac{3\pi}{32L}\left\{\cot\left(\frac{\pi}{4L}\right) + \cot\left(\frac{3\pi}{4L}\right) + \cot\left[\frac{\pi}{L}(x+1/4)\right] + \cot\left[\frac{\pi}{L}(x-1/4)\right]\right\}.$$

When $L \to \infty$, $F_L(L/2) \approx 1/2$ resulting in $S_{L/2} \approx S_\infty$. Moreover, $F_L(1) \approx 7/10$, whereas $F_L(N-1) \approx 17/42$ so that $(S_1 - S_{L/2})/S_\infty = 11/105$, in a perfect agreement with the numerical results. In fact, provided that N is larger than $10-20$, the N dependence of S_x results in the superimposition of two functions localized on $x = 1$ and $x = N$, respectively. An overlap effect occurs so that $S_{L/2} \geqslant S_\infty$. The equality holds for $L \to \infty$, only.

From the knowledge of the $\bar{\mathcal{T}}$ matrix, the diagonalization of $\mathcal{H}_{\rm po}$ is carried out numerically. In spite of the inhomogeneity of S_x, this procedure reveals that the polaron eigenstates are quite similar to stationary states defined as

$$\tilde{\omega}_\mu \approx \tilde{\omega}_0 + 2\tilde{\Phi}\cos(K_\mu), \quad |\mu\rangle \approx \sum_{x=1}^{N}\sqrt{\frac{2}{L}}\sin(K_\mu x)|x\rangle \quad (29)$$

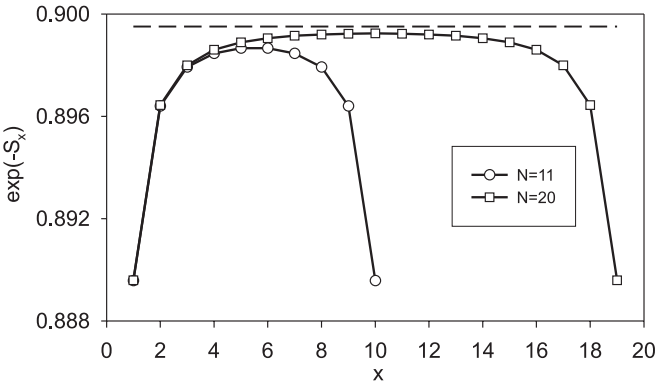

FIG. 2. $\bar{\mathcal{T}}(x,x+1)$ vs x for $C = 1.55$ and for $N = 11$ (circles), $N = 20$ (squares) and $N = \infty$ (dashed line).

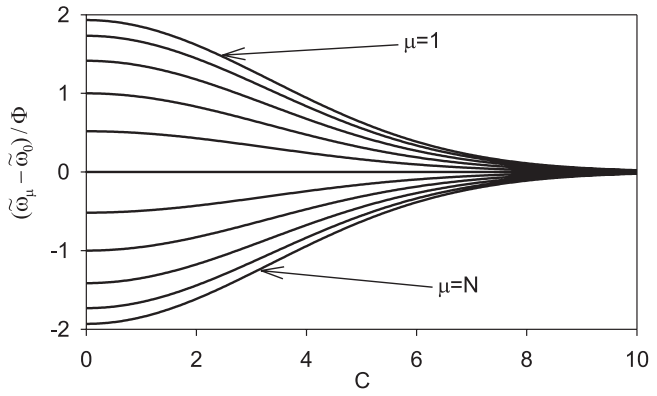

FIG. 3. Unperturbed polaronic energies $\tilde{\omega}_\mu$ vs C for $N = 11$.

with $K_\mu = \mu\pi/L$. Note that $\tilde{\omega}_{\mu=1} > \tilde{\omega}_{\mu=2} > \cdots > \tilde{\omega}_{\mu=N}$. As shown in Fig. 3, the polaron energy spectrum exhibits N discrete energy levels that belong to a band centered on $\tilde{\omega}_0$ and whose width $\sim 4\tilde{\Phi}$ decreases as C increases. The spectrum is antisymmetric with respect to the band center $[\tilde{\omega}_\mu - \tilde{\omega}_0 = -(\tilde{\omega}_{N-\mu} - \tilde{\omega}_0)]$. As a result, for odd N values, the polaron eigenstate $\mu = L/2$ is exactly located at the band center $(\tilde{\omega}_{\mu=L/2} = \tilde{\omega}_0)$.

As displayed in Fig. 4(a), each polaron eigenenergy experiences a redshift owing to the polaron-phonon interaction. This shift depends on the nature of the state. The closer to the band center the state is located, the larger is the shift. Moreover, the energy corrections do not follow a mirror symmetry and $\delta\tilde{\omega}_\mu$ slightly differs from $\delta\tilde{\omega}_{N-\mu}$. These features result from the fact that the polaron energy spectrum shows small Bohr frequencies near the band edges whereas it exhibits quite large Bohr frequencies close to the band center [Eq. (27)]. In the

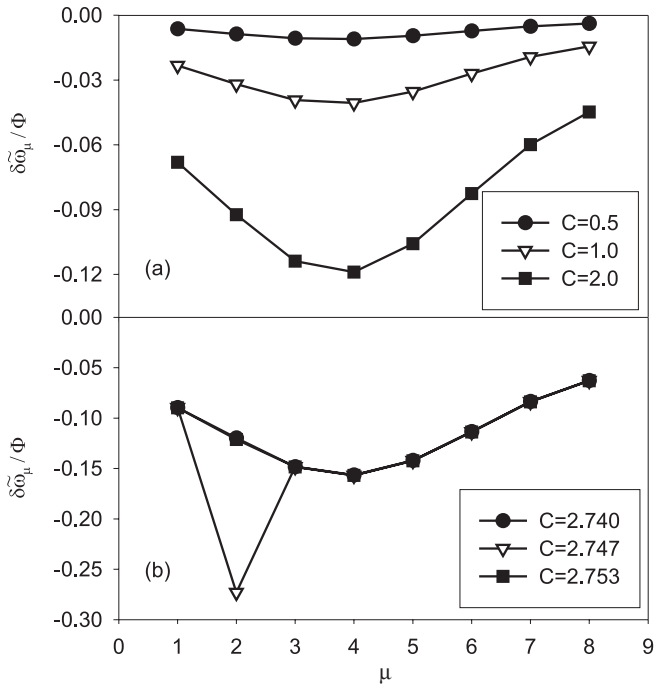

FIG. 4. Polaron energy correction $\delta\tilde{\omega}_\mu$ vs μ for $N = 8$. The corrections well behave in (a), whereas a resonance is shown in (b) (see the text).

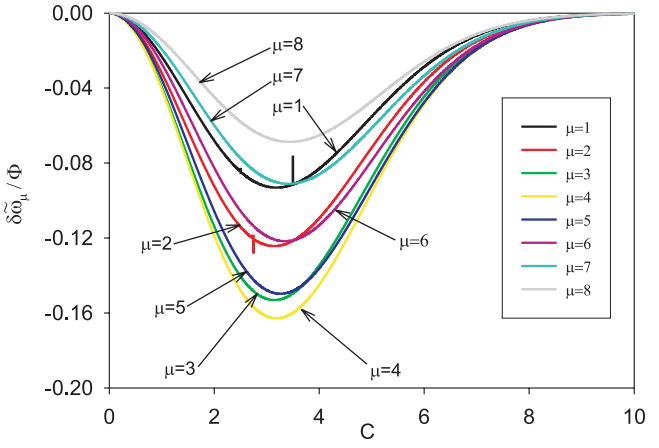

FIG. 5. (Color online) Polaron energy correction $\delta\tilde{\omega}_\mu$ vs C for $N = 8$.

weak-coupling regime, Fig. 4(a) reveals that the interaction enhances the redshift. In that case, we have verified that SE and NOE provide similar results. By contrast, for stronger couplings, SE overestimates the redshifts that become larger and larger as C increases. As shown below [Fig. 5], a different behavior is observed within NOE.

As illustrated in Fig. 4(b), NOE breaks down for critical values of the model parameters. As mentioned in Sec. V, this feature results from the occurrence of resonances between the unperturbed states coupled via $\tilde{W}_1$. For instance, a detailed analysis of $M_{p\mu\mu'}$ for $p = 1$ reveals that the interaction favors two kinds of transitions. First, it gives rise to main transitions involving neighboring states $\mu' = \mu \pm 1$ as if the states were stationary states [see Eq. (5) for $p = 1$]. Then, because of the inhomogeneity of the $\bar{T}$ matrix, the interaction allows additional transitions $\mu' = \mu \pm 3, \mu \pm 5, \ldots$ The main transitions do not induce resonances in the nonadiabatic limit. Unfortunately, this is no longer the case for the additional transitions that may favor resonances for specific values of the model parameters. For $N = 8$ and $C = 2.747$, a resonance takes place between the polaron eigenstates $\mu = 2$ and $\mu = 7$ and the phonon mode $p = 1$ so that $\tilde{\omega}_{\mu=2} - \tilde{\omega}_{\mu=7} \approx \Omega_{p=1}$. This resonance yields a singularity in the energy correction $\delta\tilde{\omega}_{\mu=2}$. However, the resonances are very sensitive to the coupling strength so that they rapidly disappear when one moves away from the critical point in parameter space.

The C dependence of the polaron energy corrections is displayed in Fig. 5 for $N = 8$. For each μ value, $\delta\tilde{\omega}_\mu$ decreases from zero as C increases. Then, it reaches a minimum for $C \approx 3.1$ whose value is approximately one order of magnitude smaller than the bare hopping constant Φ. This minimum ranges between -0.069Φ for $\mu = 8$ and -0.163Φ for $\mu = 4$. Finally, as C increases again, $\delta\tilde{\omega}_\mu$ increases and it converges to zero in the strong-coupling limit. Note that the curve $\delta\tilde{\omega}_\mu$ vs C defines a continuous function almost everywhere. Nevertheless, singularities occur for critical values of the coupling. These singularities are the signature of resonances for which NOE breaks down.

The comparison between NOE and SE is shown in Fig. 6 that displays the C dependence of $\hat{\omega}_\mu = \tilde{\omega}_\mu + \delta\tilde{\omega}_\mu$ (full lines) and $\hat{\omega}_k = \tilde{\omega}_k + \delta\tilde{\omega}_k^{(1)} + \delta\tilde{\omega}_k^{(2)}$ (dashed lines). Provided

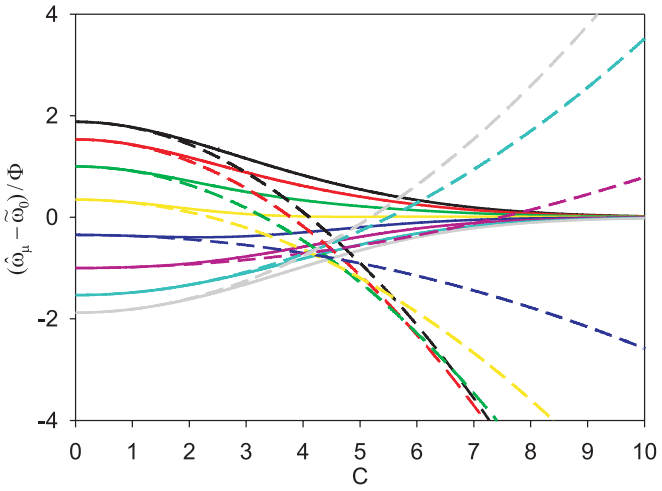

FIG. 6. (Color online) $\hat{\omega}_\mu = \tilde{\omega}_\mu + \delta\tilde{\omega}_\mu$ vs C for $N = 8$ within NOE (full lines) and SE (dashed lines).

that $C < 1$, both approaches yield similar results. However, a different behavior takes place in the intermediate- and strong-coupling regimes. Within SE, the energy corrections diverge as C increases. This is no longer the case within NOE because the energy corrections, after reaching a maximum value, vanish in the strong-coupling limit. Consequently, the corrected energies $\hat{\omega}_\mu$ form discrete energy levels that converge to $\tilde{\omega}_0$ as C increases. Theses results show that NOE is more accurate than SE almost everywhere in the parameter space. Nevertheless, although it is not well distinguishable in Fig. 6, it should be kept in mind the NOE breaks down for critical values of the model parameters.

To interpret these results, an approximate expression of $\delta\tilde{\omega}_\mu$ can be obtained by invoking simplifying assumptions. To proceed, we first suppose that the polaron eigenstates reduce to stationary waves [Eq. (29)]. Then, we restrict our attention to normal scattering processes $\mu' = \mu - p$ and $\mu' = \mu + p$, only. Consequently, Eq. (27) is expressed as a Taylor series in terms of the adiabaticity as

$$\delta\tilde{\omega}_\mu \approx -2E_B\tilde{B}^2 - \frac{8E_B\tilde{B}^3}{\pi}\cos(K_\mu) + E_B\tilde{B}^2\cos(2K_\mu) + \frac{56E_B\tilde{B}^3}{15\pi}\cos(3K_\mu), \quad (30)$$

where $\tilde{B} = B\exp(-S_\infty)$. Equation (30) reproduces the behavior observed in Figs. 4–6. It reveals that the coupling dependence is encoded in both E_B and $\exp(-S_\infty)$. This is the reason why $\delta\tilde{\omega}_\mu$ first decreases as C increases and then vanishes in the strong-coupling limit. Moreover, it shows that the interaction yields a correction to the small polaron binding energy, modifies the polaron hopping constant and induces transitions between second and third nearest neighbor sites. However, Eq. (30) does not reproduce the resonances that result from the small discrepancy between exact polaronic states and stationary waves.

As displayed in Fig. 7, the frequency of each phonon mode is either red or blue shifted owing to its interaction with a polaron. Although $\delta\Omega^{(1)}_{p\mu}$ and $\delta\Omega^{(2)}_{p\mu}$ have the same sign, it turns out that $\delta\Omega^{(2)}_{p\mu}$ is approximately one order of magnitude

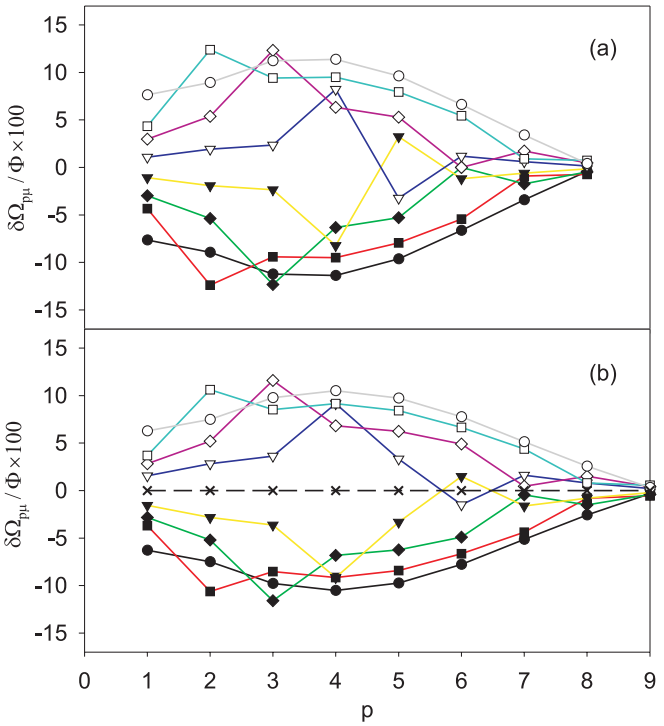

FIG. 7. (Color online) Phonon frequency shifts for $C = 2.0$ and for (a) $N = 8$ and (b) $N = 9$. (a) $\mu = 1$ (full circles), $\mu = 2$ (full squares), $\mu = 3$ (full diamonds), $\mu = 4$ (full triangles), $\mu = 5$ (open triangles), $\mu = 6$ (open diamonds), $\mu = 7$ (open squares), and $\mu = 8$ (open circles). (b) $\mu = 1$ (full circles), $\mu = 2$ (full squares), $\mu = 3$ (full diamonds), $\mu = 4$ (full triangles), $\mu = 5$ (thin x), $\mu = 6$ (open triangles), $\mu = 7$ (open diamonds), $\mu = 8$ (open squares), and $\mu = 9$ (open circles).

larger than $\delta\Omega^{(1)}_{p\mu}$. In a general, a polaron whose energy lies above $\tilde{\omega}_0$ yields a redshift of the phonon frequency whereas a polaron whose energy lies below $\tilde{\omega}_0$ favors a blue shift. The shifts are antisymmetric with respect to the polaron band center ($\delta\Omega^{(i)}_{p\mu} = -\delta\Omega^{(i)}_{pL-\mu}\ \forall i$). Nevertheless, opposite situations may appear, especially when the polaron occupies states close to the band center. For instance, for $N = 9$, the polaron in state $\mu = 4$ favors a blue shift of the frequency of the phonon mode $p = 6$, whereas the polaron in state $\mu = 5$ induces a redshift. In addition, some phonon modes remain almost insensitive to the polaron that occupies specific states. For $N = 9$, when the polaron is either in $\mu = 3$ or 7, the phonon mode $p = 7$ is only slightly perturbed. As shown in Fig. 7(b), a remarkable effect arises for odd N values. In that case, phonons dressed by a polaron whose energy is exactly located at the band center are not perturbed, i.e., $\delta\Omega^{(i)}_{p\mu=L/2} = 0\ \forall\ p$ and $\forall i$.

We have verified that SE provides phonon frequency shifts quite similar to those predicted by NOE in the weak-coupling limit ($C < 1$). However, both approaches differ as C increases. In the intermediate- and strong-coupling regimes, SE overestimates the shifts that gradually increase as C increases. As illustrated in Fig. 8 for $p = 1$, a different behavior is obtained within NOE. In absolute value, the frequency shift first increases with C from zero. Then, for $C \approx 4.8$, it reaches a maximum whose value ranges between 0.072Φ (for $\mu = 1$ and N) and 0.005Φ (for $\mu \approx L/2$). Finally, the shift decreases

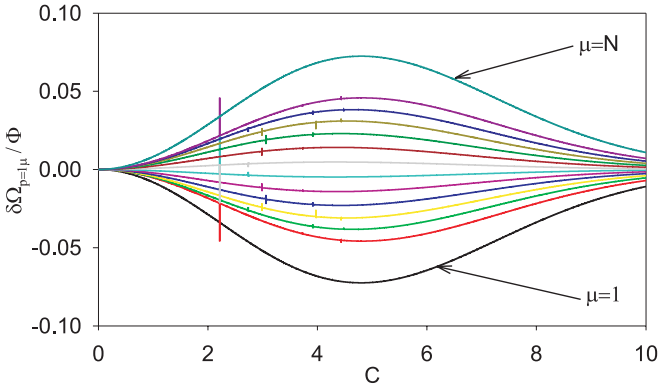

FIG. 8. (Color online) $\delta\Omega_{p=1\mu}$ vs C for $N = 14$.

in the strong-coupling regime and it tends to zero. However, the curve exhibits singularities that characterize resonances for which the method breaks down. For instance, for $N = 14$ and $C = 2.215$, two resonances have been identified. The first resonance involves the states $\mu = 2$ and 7 ($\tilde{\omega}_{\mu=2} - \tilde{\omega}_{\mu=7} \approx \Omega_{p=1}$), whereas the second resonance involves the states $\mu = 8$ and 13 ($\tilde{\omega}_{\mu=8} - \tilde{\omega}_{\mu=13} \approx \Omega_{p=1}$). Consequently, $\delta\Omega_{p=1\mu}$ takes unphysical values when the polaron occupies the states $\mu = 2$, 7, 8, or 13.

The behavior of the maximum value of the phonon frequency shift $\delta\Omega_m$ is displayed in Fig. 9. As shown in Fig. 9(a), $\delta\Omega_m$ decreases with the lattice size and it scales as $\delta\Omega_m \propto 1/L$. Therefore, the larger is the lattice size, the smaller

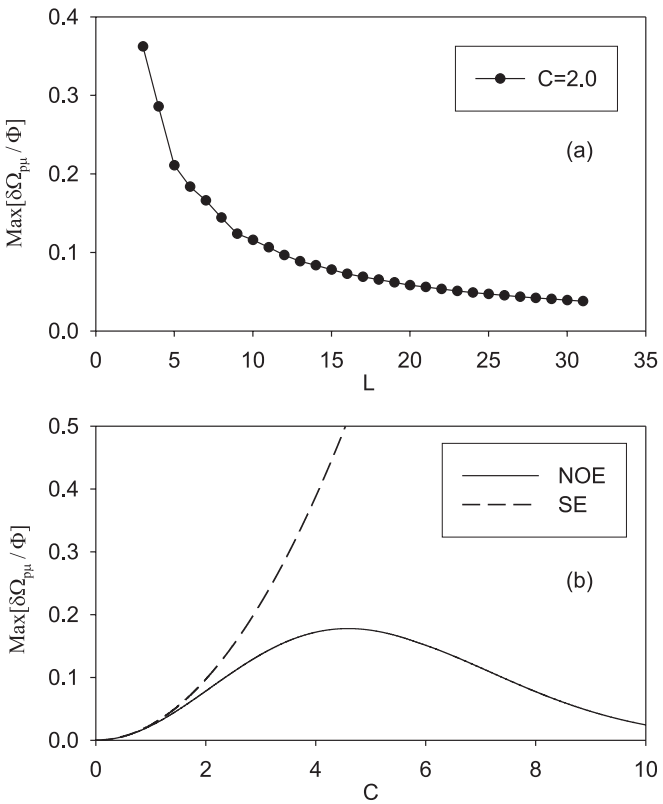

FIG. 9. (a) L dependence of the maximum phonon frequency shift for $C = 2.0$, and (b) C dependence of the maximum phonon frequency shift for $N = 14$.

is the perturbation experienced by the phonons. As illustrated in Fig. 9(b) (full line), $\delta\Omega_m$ first increases with C from zero. It reaches a maximum value $\sim 0.17\Phi$ for $C \approx 4.580$. Then, it decreases as C increases again and it tends to zero in the strong-coupling limit. By contrast, although SE works quite well in the weak-coupling limit ($C < 1.0$), it breaks down in the intermediate- and strong-coupling regimes. It predicts a shift that diverges as C increases.

To discuss this results, an approximate expression of $\delta\Omega_{p\mu}$ can be obtained by assuming that the polaron eigenstates behave as stationary states. Restricting our attention to normal scattering processes, the main contribution to the phonon frequency shift is expressed

$$\delta\Omega_{p\mu} \approx -\frac{8\tilde{B}E_B}{L}\left(\frac{\Omega_p}{\Omega_c}\right)\left[1-\left(\frac{\Omega_p}{\Omega_c}\right)^2\right]\cos(K_\mu). \quad (31)$$

Equation (31) shows that $\delta\Omega_{p\mu} < 0$ if $\mu < L/2$ whereas $\delta\Omega_{p\mu} > 0$ if $\mu > L/2$, in quite good agreement with the numerical results. It reveals that $\delta\Omega_{p\mu} = 0\ \forall\ p$ for $\mu = L/2$, as observed in Fig. 7(b). Moreover, Eq. (31) shows that $\pm\delta\Omega_m$ is the shift experienced by the phonon whose frequency is $\Omega_p = \Omega_c/\sqrt{3}$ and that is accompanied by a polaron either in state $\mu = 1$ or $\mu = N$. This maximum frequency shift is approximately $\delta\Omega_m \approx 3.08\tilde{B}E_B/L$. It scales as $1/L$, as observed in Fig. 9(a). Its coupling dependence is encoded in both E_B and $\exp(-S_\infty)$ so that it first increases as C increases and then decreases in the strong-coupling limit. Nevertheless, as Eq. (30), Eq. (31) does not reproduce the resonances.

At this step, let us point out the similarities and the differences between the present results and previous works.[51–54] Indeed, Eq. (31) is quite similar to the expression of the phonon frequency shift obtained by Ivic *et al.*[51] (see Appendix B). Nevertheless, fundamental differences occur. Indeed, Ivic and co-workers used a finite temperature mean-field theory in which the effective hopping constant is defined in terms of a temperature dependent band-narrowing factor. Moreover, a statistics was performed so that the phonon frequency shift depends on the thermal average of the population of the polaronic states. Our approach is more like a zero-temperature mean-field theory. The phonon-frequency shift originates in the polaron-phonon entanglement that arises when the system eigenstates are characterized within second-order PT. Indeed, PT is based on a unitary transformation that provides a new point of view in which the corrected energies no longer describe independent excitations.[12,13] A state $|\mu\rangle$ defines a polaron dressed by a virtual phonon cloud, whereas the number state $|\{n_p\}\rangle$ describes phonons clothed by virtual polaronic transitions. Consequently, the temperature is taken into account when dynamical processes are considered using the density matrix formalism.

To conclude, let us discuss the implication of the present work in the field of quantum decoherence. To proceed, it should be careful according to whether one consider the excitonic coherence or the polaronic coherence. Indeed, according to our previous works,[12,13] the phonon perturbation induced by a polaron is responsible for the decay of the coherence that measures the ability of the polaron to develop a superimposition between the vacuum and a one-polaron state $|\mu\rangle$. The corresponding decay rate is approximately

$\Gamma_\mu \approx (\sum_{p=1}^{N} \Delta\bar{n}_p^2 \delta\Omega_{p\mu}^2)^{1/2}$, where $\Delta\bar{n}_p^2 = \bar{n}_p(\bar{n}_p + 1)$ measures the thermal fluctuations of the pth phonon number around its average value $\bar{n}_p$. From Fig. 7, it turns out that the closer to the band center the polaron state is located, the smaller is Γ_μ and the slower is the decoherence. In particular, for odd lattice sizes, the coherence of the state located at the band center ($\mu = L/2$) survives over an infinite time scale because $\delta\Omega_{p\mu=L/2} = 0\ \forall p$.

By contrast, it would be premature to discuss the behavior of the excitonic coherences. Indeed, these coherences will depend on the phonon frequency shifts but also on the dressing operators. This latter dependence originates in the LF transformation that links both the original point of view and the polaron point of view. In the weak-coupling limit, the influence of the dressing operators will remain small so that excitonic coherences will behave as polaronic coherences. However, it will no longer be the case in the intermediate- and strong-coupling regimes. A detailed study is thus required and it will be addressed in a forthcoming paper.

VII. CONCLUSION

In the present paper, the finite-size exciton-phonon system has been revisited within the small polaron theory. Based on LF transformation, a new point of view was generated in which a polaron defines an exciton dressed by a lattice distortion. When the polaron is immobile, its frequency is red shifted by an amount that depends on the lattice size, whereas the phonon frequencies remain unchanged. However, when the polaron is allowed to move, a polaron-phonon interaction occurs. It favors polaronic transitions between neighboring sites, either freely or through phonon exchanges. Two strategies have thus been proposed to treat this interaction.

Within SE, the interaction is expanded as a Taylor series with respect to the coupling strength. At zero order, the expansion reduces to the kinetic energy of a bare exciton. It was used to define a polaron Hamiltonian whose eigenstates correspond to stationary waves. Therefore, high-order contributions describe polaron scattering mediated by the exchange of real and virtual phonons, the latter resulting from phonon vacuum fluctuations. Up to second order, PT has been applied for characterizing polaron energy corrections and phonon-frequency shifts. Quite surprisingly, it turned out that SE does not improve energy calculations when compared with PT applied in the exciton-phonon point of view.

Within NOE, the interaction is expanded as a Taylor series involving normally ordered terms. Each term describes polaron scattering mediated by the exchange of real phonons, only. The scattering strength is renormalized up to infinity by taking into account exactly of the phonon vacuum fluctuations. The polaron Hamiltonian is thus defined in terms of inhomogeneous effective hopping constants so that the polaronic eigenstates slightly differ from stationary waves. It has been shown that NOE is more accurate than SE, especially in the intermediate- and strong-coupling regimes. The interaction yields a redshift of the polaron frequency. It modifies the effective hopping constants and favors transitions between second and third nearest neighbor sites. Similarly, each phonon experiences a frequency shift when it is accompanied by a polaron. This effect is an intrinsic property of a confined lattice because the larger is the lattice size the smaller is the shift. It turns out that the interaction yields either the softening or the hardening of the phonon frequency, depending on the state occupied by the polaron. However, for odd lattice sizes, the phonon frequencies remain unchanged when the polaron occupies the state exactly located at the band center. Unfortunately, it has been observed that NOE breaks down for critical values of the model parameter. Because polaronic eigenstates differ from stationary states, additional scattering processes are allowed. These processes may conserve the energy resulting in the occurrence of resonances at the origin of divergences in the energy corrections.

Through this paper, we have identified the strengths and weaknesses of NOE. Consequently, in forthcoming works, we shall first develop a more efficient formalism to overcome the problems induced by the resonances. Then, NOE will be applied to simulate dynamical processes at finite temperature. Special attention will be paid for describing excitonic coherences as well as QST in the intermediate- and strong-coupling regimes.

APPENDIX A: NORMAL ORDERING OF THE INTERACTION

In the local basis, the polaron-phonon interaction is written as

$$\tilde{V} = \sum_{x=1}^{N-1} \Phi(\theta_{x+1}^\dagger \theta_x |x+1\rangle\langle x| + \theta_x^\dagger \theta_{x+1} |x\rangle\langle x+1|). \tag{A1}$$

Using Glauber-Weyl formula,[55] the product involving dressing operators is normally ordered as

$$\begin{aligned} \theta_{x+1}^\dagger \theta_x &= e^{-\sum_p \frac{1}{2}\lambda_{px}^2} e^{+\sum_p \lambda_{px} a_p^\dagger} e^{-\sum_p \lambda_{px} a_p}, \\ \theta_x^\dagger \theta_{x+1} &= e^{-\sum_p \frac{1}{2}\lambda_{px}^2} e^{-\sum_p \lambda_{px} a_p^\dagger} e^{+\sum_p \lambda_{px} a_p}, \end{aligned} \tag{A2}$$

where $\lambda_{px} = \Lambda_{px+1x+1} - \Lambda_{pxx}$. Therefore inserting Eq. (A2) into Eq. (A1) and expanding the exponentials as a Taylor series, $\tilde{V}$ is written as $\tilde{V} = \sum_{m=0}^{\infty} \tilde{W}_m$, $\tilde{W}_m$ being defined as

$$\begin{aligned} \tilde{W}_m = {} & \frac{\Phi}{m!} \sum_{p_1=1}^{N} \cdots \sum_{p_m=1}^{N} \sum_{x=1}^{N} e^{-\sum_p \frac{1}{2}\lambda_{px}^2} \lambda_{p_1 x} \cdots \lambda_{p_m x} |x+1\rangle \\ & \times \langle x| \sum_{r=0}^{m} (-1)^r \binom{m}{r} a_{p_1}^\dagger \cdots a_{p_{m-r}}^\dagger a_{p_{m-r+1}} \cdots a_{p_m} \\ & + \frac{\Phi}{m!} \sum_{p_1=1}^{N} \cdots \sum_{p_m=1}^{N} \sum_{x=1}^{N} e^{-\sum_p \frac{1}{2}\lambda_{px}^2} \lambda_{p_1 x} \cdots \lambda_{p_m x} |x\rangle \\ & \times \langle x+1| \sum_{r=0}^{m} (-1)^{m-r} \binom{m}{r} a_{p_1}^\dagger \cdots a_{p_{m-r}}^\dagger a_{p_{m-r+1}} \cdots a_{p_m}. \end{aligned} \tag{A3}$$

This equation can be expressed in a more useful form that does not depend on the nature of the polaronic basis. To proceed, it should first be noted that the λ_{px} coefficients yield

the occurrence of the coupling operators as

$$\lambda_{px}|x+1\rangle\langle x| = [\Lambda_p, |x+1\rangle\langle x|],$$
$$\lambda_{px}|x\rangle\langle x+1| = -[\Lambda_p, |x\rangle\langle x+1|]. \quad \text{(A4)}$$

Then the sum over x simplifies through the introduction of the effective transfer matrix Eq. (23). After simple algebraic manipulations, one finally obtains Eqs. (21) and (22). Note that the double dot operation can be used because $\tilde{W}_{m,p_1p_2\ldots p_m}$ is invariant under the $m!$ permutations over the indexes $p_1, p_2, \ldots, p_m$.

APPENDIX B: COMPARISON WITH THE WORKS OF IVIC AND CO-WORKERS

In a translationally invariant lattice containing N sites, Ivic and co-workers used a finite temperature mean-field procedure for characterizing the modifications of the phonon spectra induced by the polaron-phonon interaction.[51–54] They showed that the frequency of the phonon mode with wave vector q and harmonic frequency $\Omega_q = \Omega_c|\sin(q/2)|$ is defined as

$$\tilde{\Omega}_q^2 = \Omega_q^2(1+\mathcal{F}_q), \quad \text{(B1)}$$

where $\mathcal{F}_q$ is expressed as

$$\mathcal{F}_q = -\frac{8B|F_q|^2 e^{-S(T)}}{\Omega_c\Omega_q}\frac{1}{N}\sum_K n_K\cos(K). \quad \text{(B2)}$$

In Eq. (B2), $|F_q| = [2E_B\Omega_q(1-(\Omega_q/\Omega_c)^2)]^{1/2}$ is the coupling strength, $S(T)$ is the so-called temperature dependent band-narrowing factor and n_K is the small-polaron mean number in the Bloch state with wave vector K. In the nonadiabatic limit, i.e., provided that $B \ll 1$, Eq. (B1) simplifies and one obtains $\tilde{\Omega}_q = \Omega_q + \delta\Omega_q$ with

$$\delta\Omega_q \approx -\frac{8\tilde{B}E_B}{N}\left(\frac{\Omega_q}{\Omega_c}\right)\left[1-\left(\frac{\Omega_p}{\Omega_c}\right)^2\right]\times\sum_K n_K\cos(K),$$

where $\tilde{B} = B\exp[-S(T)]$. As discussed in Sec. VI, this equation basically reduces to Eq. (31) at zero temperature [$S(T) = S_\infty$] and when a specific polaronic Bloch state K is occupied ($n_{K'} = \delta_{KK'}$). Size effects arise through the quantization of both the phonon wave vector and the polaron wave vector. Nevertheless, this equation remains too simple to capture all the features displayed in Figs. 7, 8, and 9.

*vincent.pouthier@univ-fcomte.fr

[1] C. H. Bennet and D. P. DiVincenzo, Nature (London) **404**, 247 (2000).
[2] D. Burgarth, V. Giovannetti, and S. Bose, Phys. Rev. A **75**, 062327 (2007).
[3] O. Mandel, M. Greiner, A. Widera, T. Rom, T. W. Hansch, and I. Bloch, Nature (London) **425**, 937 (2003).
[4] D. Loss and D. P. DiVincenzo, Phys. Rev. A **57**, 120 (1998).
[5] S. Bose, Phys. Rev. Lett. **91**, 207901 (2003).
[6] M. Christandl, N. Datta, T. C. Dorlas, A. Ekert, A. Kay, and A. J. Landahl, Phys. Rev. A **71**, 032312 (2005).
[7] C. M. Tesch and R. de Vivie-Riedle, Phys. Rev. Lett. **89**, 157901 (2002).
[8] C. Tesch and R. de Vivie-Riedle, J. Chem. Phys. **121**, 12158 (2004).
[9] C. Gollub and R. de Vivie-Riedle, Phys. Rev. A **78**, 033424 (2008).
[10] C. Gollub, Ph.D. thesis, Ludwig Maximilian University of Munich, 2009.
[11] M. B. Plenio, J. Hartley, and J. Eisert, New J. Phys. **6**, 36 (2004).
[12] V. Pouthier, Phys. Rev. B **83**, 085418 (2011).
[13] V. Pouthier, J. Chem. Phys. **134**, 114516 (2011).
[14] H. Fröhlich, Adv. Phys. **3**, 325 (1954).
[15] B. N. J. Persson, Phys. Rev. B **46**, 12701 (1992).
[16] V. Pouthier and C. Girardet, Phys. Rev. B **60**, 13800 (1999).
[17] M. Bonn, M. C. Hess, and M. Wolf, J. Chem. Phys. **115**, 7725 (2001).
[18] V. Pouthier, J. C. Light, and C. Girardet, J. Chem. Phys. **114**, 4955 (2001).
[19] P. Jakob, J. Chem. Phys. **114**, 3692 (2001).
[20] V. Pouthier and C. Girardet, Phys. Rev. B **65**, 035414 (2001).
[21] V. Pouthier, J. Chem. Phys. **118**, 3736 (2003).
[22] W. G. Roeterdink, O. Berg, and M. Bonn, J. Chem. Phys. **121**, 10174 (2004).
[23] V. Pouthier, Phys. Rev. B **71**, 115401 (2005).
[24] V. Pouthier, Phys. Rev. B **74**, 125418 (2006).
[25] A. S. Davydov and N. I. Kisluka, Phys. Status Solidi **59**, 465 (1973); Zh. Eksp. Teor. Fiz. **71**, 1090 (1976) [Sov. Phys. JETP **44**, 571 (1976)].
[26] A. C. Scott, Phys. Rep. **217**, 1 (1992).
[27] D. W. Brown and Z. Ivic, Phys. Rev. B **40**, 9876 (1989).
[28] Z. Ivic, D. Kostic, Z. Przulj, and D. Kapor, J. Phys. Condens. Matter **9**, 413 (1997).
[29] V. Pouthier, Phys. Rev. E **68**, 021909 (2003).
[30] J. Edler, R. Pfister, V. Pouthier, C. Falvo, and P. Hamm, Phys. Rev. Lett. **93**, 106405 (2004).
[31] C. Falvo and V. Pouthier, J. Chem. Phys. **123**, 184709 (2005); **123**, 184710 (2005).
[32] D. Tsivlin and V. May, Chem. Phys. **338**, 150 (2007).
[33] P. A. S. Silva and L. Cruzeiro, Phys. Rev. E **74**, 021920 (2006).
[34] V. Pouthier and Y. O. Tsybin, J. Chem. Phys. **129**, 095106 (2008).
[35] V. Pouthier, Phys. Rev. E **78**, 061909 (2008).
[36] V. Pouthier, J. Phys. Condens. Matter **21**, 185404 (2009).
[37] V. Pouthier, Phys. Rev. B **79**, 214304 (2009).
[38] V. Pouthier, J. Chem. Phys. **132**, 035106 (2010).
[39] V. Pouthier, Phys. Rev. E **81**, 031913 (2010).
[40] E. R. Bittner, A. Goj, and I. Burghardt, Chem. Phys. **370**, 137 (2010).
[41] V. Pouthier, J. Phys. Condens. Matter **22**, 385401 (2010).
[42] M. Schlosshauer, *Decoherence and the Quantum-to-Classical Transition* (Spinger-Verlag, Berlin, 2007).
[43] H. P. Breuer and F. Petruccione, *The Theory of Open Quantum Systems* (Oxford University Press, New York, 2007).
[44] V. Pouthier, J. Phys. Condens. Matter **22**, 255601 (2010).
[45] G. D. Mahan, *Many-Particle Physics* (Plenum, New York, 1990).

[46]A. S. Alexandrov and J. T. Devreese, *Advances in Polaron Physics* (Springer-Verlag, Berlin, 2010).
[47]A. S. Alexandrov, Phys. Rev. B **61**, 12315 (2000).
[48]I. G. Lang and Yu. A. Firsov, Sov. Phys. JETP **16**, 1293 (1962).
[49]A. S. Alexandrov and H. Capellmann, Phys. Rev. B **43**, 2042 (1991).
[50]J. Ranninger, Phys. Rev. B **48**, 13166 (1993).
[51]Z. Ivic, G. Vujicic, and Z. Przulj, Phys. Lett. A **316**, 126 (2003).
[52]Z. Ivic, S. Zekovic, D. Cevizovic, and D. Kostic, Physica B **355**, 417 (2005).
[53]Z. Ivic, S. Zekovic, D. Cevizovic, D. Kostic, and G. Vujicic, Physica B **362**, 187 (2005).
[54]D. Cevizovic, S. Zekovic, Z. Ivic, and Z. Przulj, Phys. Lett. A **358**, 457 (2006).
[55]W. Witschel, Eur. J. Phys. **17**, 357 (1996).